



Enhancing Target Detection and Recognition in Advanced Driver Assistance Systems Using Infrared Thermal Imaging and the YOLOv5 Algorithm

Mingxia Zhong¹, Bojun Jiang^{2*}

¹ School of Electronic Commerce, Zhejiang Business College, Hangzhou 310059, China

² School of Applied Engineering and Technology, Zhejiang Business College, Hangzhou 310059, China

Corresponding Author Email: 00222@zjbc.edu.cn

Copyright: ©2024 The authors. This article is published by IIETA and is licensed under the CC BY 4.0 license (<http://creativecommons.org/licenses/by/4.0/>).

<https://doi.org/10.18280/ijht.420530>

ABSTRACT

Received: 17 May 2024

Revised: 10 August 2024

Accepted: 25 September 2024

Available online: 31 October 2024

Keywords:

Advanced Driving Assistance System (ADAS), automotive sensor, infrared thermal imaging, target detection, YOLOv5 algorithm, deep learning, low-visibility condition

The potential of Advanced Driving Assistance Systems (ADAS) to enhance road safety is considerable; however, the reliability of ADAS in detecting and classifying road entities under varied environmental conditions remains a critical challenge. Conventional ADAS sensors often encounter limitations in adverse weather and low-visibility conditions, such as nighttime, rain, snow, and haze, reducing their capacity to detect vehicles and pedestrians effectively. To address these limitations, this study explores the integration of infrared thermal imaging technology into standard automotive sensor kits to enhance target detection capabilities. The YOLOv5 deep learning algorithm is applied to infrared thermal imaging data, aiming to improve the detection and classification of road targets, including pedestrians and motor vehicles, across diverse driving scenarios. Experimental results demonstrate that the proposed approach significantly enhances target detection, maintaining a balance between detection accuracy and real-time performance, particularly under challenging visibility conditions. These findings indicate that the integration of infrared thermal imaging with YOLOv5 in ADAS could reduce accident risks and improve road safety by providing more reliable scene analysis under adverse conditions.

1. INTRODUCTION

ADAS [1] detects and identifies objects using an array of vehicle-mounted sensors, including millimeter-wave radar, LiDAR, ultrasound, and visible-light cameras. During vehicle operation, these sensors assess distances to nearby vehicles and pedestrians, gather traffic data, and monitor road signs. Combined with navigation maps, ADAS enables real-time identification, dynamic tracking, and classification of traffic objects, such as pedestrians and motor vehicles, thereby supporting early warning systems and assisting drivers in maintaining safe driving practices through systematic data processing and analysis [2]. Target detection is considered a core component of ADAS [3], as it relies on integrated sensors, processing units, and control mechanisms to help drivers anticipate potential hazards, mitigate human error, counteract distractions, and reduce accident rates. As an active safety technology, target detection is critical to improving road safety. The process of object detection in ADAS primarily comprises two key stages: (1) sensing, or perceiving, target objects; and (2) classifying objects to inform subsequent actions. In the first stage, sensing technology enhances or even substitutes human perception, optimising vehicle performance in diverse driving scenarios. The second stage involves classifying and recognising traffic-related images or video data captured by sensors through deep-learning algorithms. This classification enables the system to differentiate between various traffic objects, including motor vehicles, pedestrians, and bicycles,

thereby refining target recognition and response capabilities.

In complex driving environments, however, target detection remains a considerable challenge. The limitations of current ADAS sensors and detection algorithms can affect system performance. The predominant sensors in ADAS, including visible-light cameras, radar, and laser rangefinders, present unique constraints. While visible-light cameras [4] capture high-resolution environmental data and perform effectively under sufficient lighting for tasks such as lane departure warnings, emergency braking assistance, and pedestrian and animal detection, their night-vision capabilities are limited, and visibility deteriorates in adverse weather. LiDAR sensors [5], capable of acquiring three-dimensional environmental information, also face drawbacks. Although effective for obstacle avoidance when combined with other sensors, LiDAR performance declines in dusty, rainy, and foggy conditions, with recognition accuracy diminished, particularly for smaller objects. Object detection based on deep-learning algorithms has progressed significantly in recent years, with prominent algorithms such as Faster R-CNN [6, 7], YOLO [8, 9], and SSD [10] demonstrating considerable efficacy in vehicle and pedestrian detection as well as in traffic sign recognition. Despite these advancements, challenges persist, particularly in complex environments or under low-light and adverse weather conditions, where deep-learning algorithms may produce false detections or fail to detect targets entirely. Moreover, real-time performance demands are not consistently met, impacting the timeliness and reliability of

2. THE ADVANTAGES OF INFRARED THERMAL IMAGING TECHNOLOGY

2.1 Strong night vision ability

Pedestrians, as critical participants in traffic and the most vulnerable road users, are particularly important to detect in complex traffic environments within ADAS systems. The report released by the Governor's Highway Safety Association (GHSA) shows that the growth rate of pedestrian fatalities in the United States has been much faster in recent years than all other traffic fatalities [11]. In the first half of 2022, approximately 3,500 pedestrians were killed in the U.S., equating to one pedestrian fatality every 75 minutes—a 5% increase over the same period in 2021. Over the past three years, the number of pedestrian deaths in the U.S. has risen by 18%, a rate nine times faster than that of the general population

growth. According to research by the International Commission on Illumination (CIE), the traffic accident rate at night is three times higher than during the day. Insufficient road lighting has been identified as a primary factor impacting driver safety at night, with traffic accidents occurring during nighttime accounting for approximately 40% of all accidents but resulting in a high fatality rate of up to 60%. These statistics indicate that the risk of driving at night is considerably higher than during daylight hours [12], underscoring the importance of night vision capabilities in ADAS systems for effective pedestrian and vehicle detection.

The ADAS market has expanded rapidly in recent years. While sensor technology continues to advance, no single sensor can ensure absolute driving safety, as each sensor type presents distinct advantages and limitations. Table 1 below summarizes the applications of various sensors in ADAS-assisted driving. It is evident that, compared to other sensors, infrared thermal imaging technology not only excels in pedestrian detection and classification but also provides unique advantages in night vision capabilities [13].

Table 1. The corresponding detection application of different sensors in ADAS system

| Application | Visible | Thermal | Radar | LIDAR | Ultrasound |
|---------------------------|---------|---------|-------|-------|------------|
| Traffic Sign Recognition | √ | | | | |
| Adaptive Cruise Control | | √ | | | |
| Lane Departure Warning | √ | | | | |
| Front Cross Traffic Alert | | √ | | | √ |
| Emergency Brake Assist | √ | √ | √ | | √ |
| Pedestrian Detection | √ | | √ | | √ |
| Pedestrian Classification | √ | | | | √ |
| Night Vision | | | | | √ |
| Blind Spot Detection | | √ | | √ | √ |
| Rear Collision Warning | | √ | | | |
| Park Assist | √ | | | √ | |
| Rear Cross Traffic Alert | | √ | | √ | √ |
| Rear AEB | | | | √ | |
| Collision Avoidance | √ | √ | √ | | √ |
| Surround View | √ | | | | √ |

2.2 Long operating range, with a detection range four times that of regular headlights

The infrared thermal imager operates continuously, providing 24-hour functionality, and benefits from the strong atmospheric transmissivity of thermal radiation. As a result, thermal imaging is particularly advantageous for nighttime observation and offers an extended detection range [14]. In Figure 1, the left image shows an RGB camera capture taken with high-beam illumination on a night road, while the right image presents an infrared thermal image of the same location. Unlike the RGB camera, the thermal imager is unaffected by ambient and artificial lighting conditions and can detect objects at a range four times greater than the high beam's illumination distance.



Figure 1. Comparison of RGB image and infrared thermal imager imaging effects under night road conditions

2.3 Eliminate glare and weather interference

In harsh weather conditions, such as rain, snow, and haze, visible-light cameras produce images with low visibility, indistinct target boundaries, or targets that blend into the background, making them unsuitable for effective object detection and recognition. By contrast, thermal infrared or long-wave infrared cameras are capable of detecting and classifying targets in darkness or dense fog and are unaffected by solar glare, thereby enhancing situational awareness [15]. As illustrated in Figure 2, testing conducted in a haze-filled tunnel demonstrated that the visibility of the infrared thermal imaging camera (right) was significantly higher than that of the visible-light camera (left), making it more appropriate for image preprocessing applications.

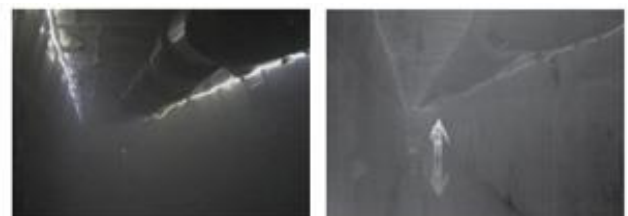


Figure 2. Comparison of visible light camera images and thermal imaging camera images in haze tunnels

2.4 Sensitive to temperature

Due to limitations in their working principles, typical sensors such as visible-light cameras, LiDAR, and radar are affected by target reflectivity and atmospheric conditions, which can impact their performance. In contrast, infrared thermal imaging technology leverages the fact that all objects emit thermal energy, thereby removing the need for external reference sources. This technology is highly sensitive to temperature differences, enabling clear visualisation of objects in the environment. As demonstrated in Figure 3, an example presented at the SIA Vision 2016 conference [16] compares images captured by a visible-light RGB camera and a long-wave infrared (LWIR) thermal imaging camera in a fog-filled tunnel. It is evident that the LWIR images facilitate superior target recognition under such conditions.



Figure 3. Example images recorded in fog tunnel with thermal (LWIR), visible RGB

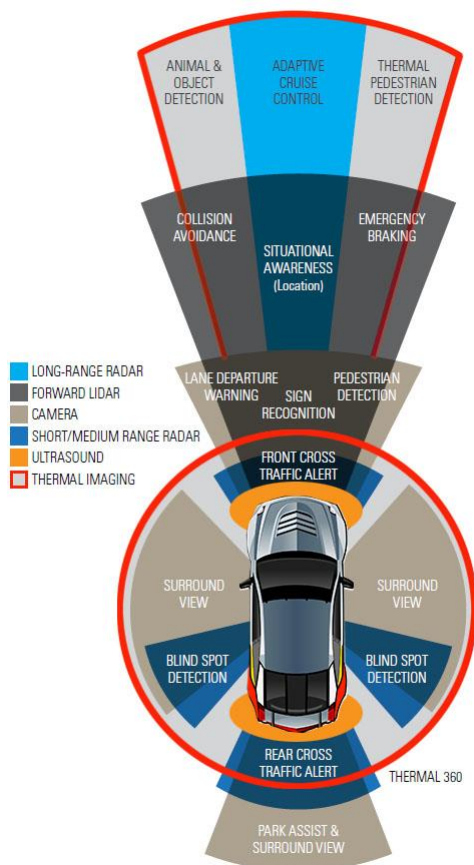


Figure 4. Sensing kits in ADAS and AV platforms using infrared thermal imaging technology

In summary, as an integral sensor within onboard ADAS systems, accurate sensing across diverse and complex environments typically requires the fusion and complementary use of multiple sensors to deliver a more comprehensive and

precise target recognition solution for autonomous driving. Sensor fusion technology thus represents a critical component in achieving full vehicle intelligence in the future. The inclusion of an infrared thermal imager in the sensor kit of a vehicle is essential. The application of infrared thermal imaging technology enhances the reliability of the ADAS sensor suite and improves overall system perception performance. Figure 4 illustrates the expanded object detection capability and range achieved by augmenting traditional sensor kits with infrared thermal imaging technology [17].

3. INFRARED THERMAL IMAGE PREPROCESSING

As discussed previously, while infrared thermal imaging technology (hereinafter referred to as "infrared thermal imaging") offers advantages over RGB visible-light imaging for traffic object detection, it also presents certain limitations. Infrared thermal images typically exhibit a lower signal-to-noise ratio, fewer target texture features, and lower resolution compared to visible-light images. Additionally, noise is introduced during the digital imaging process, making it challenging to distinguish between targets and the background [18]. These factors can reduce the accuracy of target detection, necessitating image preprocessing tailored to the specific characteristics of infrared thermal images. The goals of preprocessing are to reduce irrelevant noise, enhance the contrast between traffic targets and environmental backgrounds, improve the detectability of traffic targets, simplify image data, and facilitate feature extraction, thereby laying a solid foundation for subsequent detection and classification tasks [19]. Image preprocessing for infrared thermal imaging in target detection primarily involves three key aspects.

3.1 Image denoising

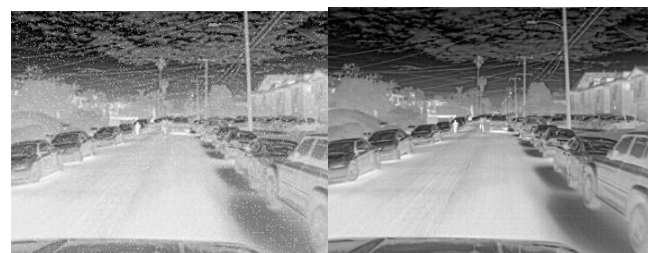


Figure 5. Comparison of infrared image denoising effects

Infrared thermal images frequently contain substantial noise, stemming partly from equipment-based sources—such as thermal noise, three-particle noise, and photon noise—due to limitations in infrared detector hardware, and partly from environmental noise. Based on an analysis of the types and characteristics of noise in infrared thermal images, this study explores the application of mathematical morphology filtering for infrared image noise reduction. It was observed that when a single structural element is employed in the open-close filter, residual negative pulse noise remains after positive pulse noise is removed; conversely, in the close-open filter, positive pulse noise remains after the removal of negative pulse noise. Furthermore, as the structural element size increases, these residual effects become more pronounced. To address this, a denoising algorithm based on multi-scale structural operator

morphological filtering is proposed, aimed at preserving the fine details of the image while effectively eliminating noise. This approach enhances the suitability of infrared images for subsequent object detection and classification tasks. The denoising results for infrared images are shown in Figure 5 [20].

3.2 Image enhancement

The primary objective of image enhancement is to increase the contrast between targets and the background in infrared thermal images. To address the low signal-to-noise ratio and resolution challenges inherent in these images, an analysis of current mainstream image enhancement methods was conducted based on the unique characteristics of infrared data. Consequently, a channel expansion-based infrared image enhancement algorithm was implemented [21]. This algorithm capitalises on the fact that infrared images are typically single-channel and therefore contain limited information. To enrich the data, two infrared image enhancement techniques—CLAHE (Contrast Limited Adaptive Histogram Equalization) and a conversion-based enhancement method—are applied to expand the single-channel infrared image into three channels, enabling it to be used in subsequent processing steps. This expansion increases the data volume and allows the network to learn a richer set of features. The results of this image enhancement process are shown in Figure 6.



Figure 6. Comparison of image enhancement effects

3.3 Target ROI extraction

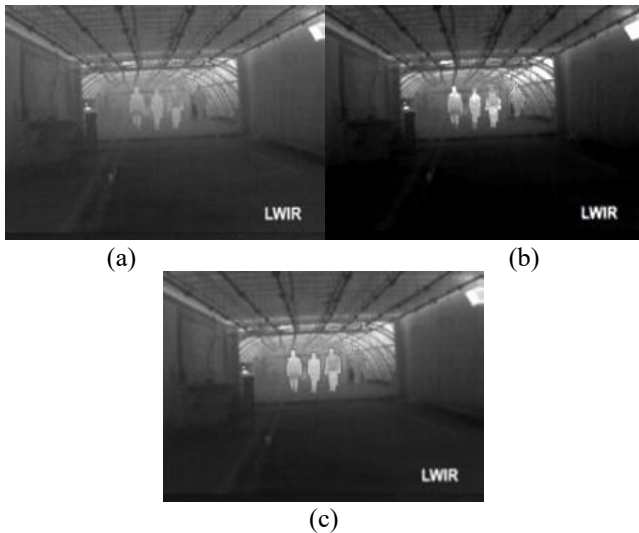


Figure 7. (a) Comparison of image enhancement effects (b) Visual saliency map (c) Target ROI extraction

Through research, it has been observed that visual saliency algorithms exhibit strong recognition performance in the domains of moving object tracking and recognition.

Consequently, this study aims to employ the principle of visual saliency for the rapid localisation of target regions of interest (ROI). However, pedestrians or distant vehicles often appear as weak infrared targets in traffic images or videos captured by infrared thermal imaging cameras. The presence of image noise or low contrast can significantly impact detection accuracy, leading to a high false detection rate. To mitigate this issue, a visual saliency algorithm based on spatial distance enhancement, as outlined in reference [22], is adopted. This method reduces noise and background interference, effectively lowering the computational complexity of the image while enhancing detection results for small infrared targets. For instance, taking the infrared thermal image from a fog tunnel shown in Figure 3 of this study (Figure 7(a)), the target ROI extraction using the spatial distance-enhanced visual saliency algorithm is illustrated in Figure 7(c).

The main process of image preprocessing is shown in Figure 8.

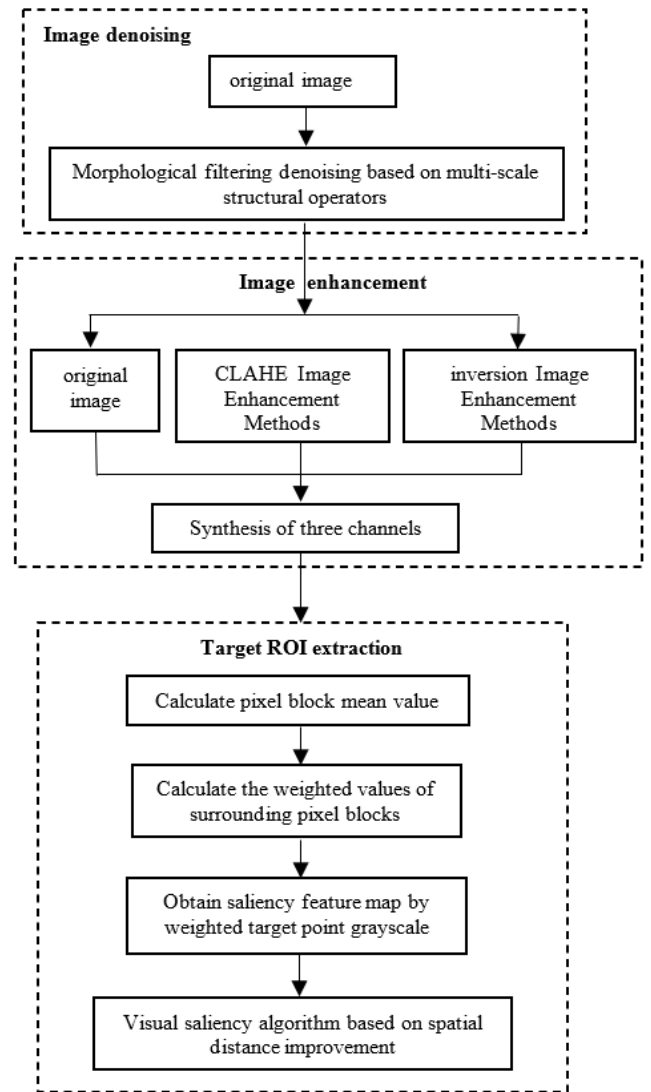


Figure 8. Image preprocessing

4. YOLOv5 TRAINING TARGET DETECTION NETWORK

Detection and classification are fundamental performance indicators in the ADAS sensor suite. The objective of traffic

object detection within an ADAS system is to identify the presence of specific types of traffic objects (e.g., pedestrians, motor vehicles, bicycles, animals, etc.) based on images or videos transmitted by the system's sensors. If an object is detected and its existence confirmed, a bounding box is returned to annotate the spatial position and coverage area of the identified object. In the context of object detection for automotive driving scenarios, it is typically required to detect multiple object types simultaneously. However, several challenges arise due to factors such as scale variations, diverse postures, complex backgrounds, and occlusion of objects within the scene. The primary challenge lies in the time-consuming nature of the template matching process following network model training, which hampers the ability to develop a target detection system that effectively balances detection accuracy and real-time performance.

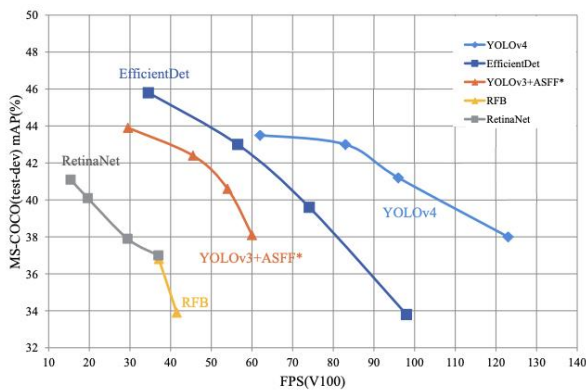


Figure 9. Performance comparison of different target detection algorithms

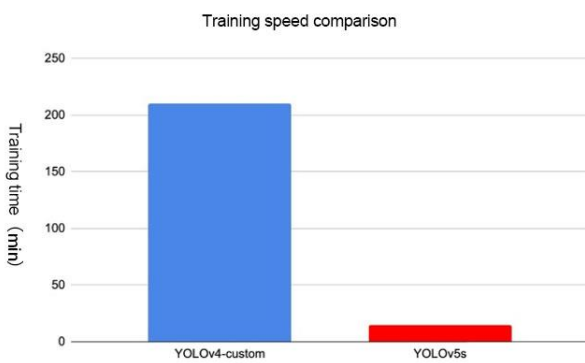


Figure 10. Comparison of training speeds between YOLO4 and YOLO5 on the same dataset

Experimental results have demonstrated that the YOLOv4 algorithm outperforms other object detection algorithms. For instance, using the MS COCO dataset, YOLOv4 achieves nearly double the detection speed (FPS) compared to the EfficientDet algorithm under similar accuracy requirements. In comparison to YOLOv3, YOLOv4 shows a 10% improvement in mAP (mean average precision), while the FPS increases by 12%, as depicted in Figure 9. With advancements in the YOLO algorithm, research conducted by the computational vision startup Roboflow reveals that YOLOv5 significantly outpaces YOLOv4 in terms of speed, as shown in Figure 10. YOLOv5 not only excels in computational performance but is also easy to configure in various hardware

environments and boasts a rapid model training speed, making it suitable for real-time system batch processing. Given the need to balance detection accuracy and real-time performance, this study employs the YOLOv5 algorithm to process the experimental dataset. This involves applying denoising, enhancement, and ROI extraction techniques on the pre-processed images, followed by transfer learning.

Transfer learning, by leveraging pre-trained model parameters from the COCO dataset within the YOLOv5 framework, accelerates model training and optimizes learning efficiency. This approach reduces the dependency on sample size and improves the model's accuracy. The process includes the following steps:

4.1 Collection and annotation of training datasets

To validate the experimental results, the FLIR Thermal Starter Dataset V1.3, released by FLIR Systems in August 2019 for algorithm training, is utilized. This dataset is derived from RGB cameras and thermal imaging cameras installed on vehicles. It consists of a total of 14,452 infrared images, including 10,228 images from multiple short videos and 4,224 images from a 144-second long video. The dataset contains five categories of target objects: pedestrians, dogs, motor vehicles, bicycles, and other vehicles. Annotations are provided in MSCOCO label vector format, offering both annotated thermal images and corresponding non-annotated RGB images, as illustrated in Figure 11. The dataset is available in five file formats: (1) 14-bit TIFF thermal images (without automatic gain control, AGC); (2) 8-bit JPEG thermal images (with AGC) without embedded bounding boxes; (3) 8-bit JPEG thermal images (with AGC) containing embedded bounding boxes for easier visualization; (4) RGB 8-bit JPEG images; and (5) JSON comments in MSCOCO format.



Figure 11. FLIR thermal starter dataset image example (a) RGB visible light image (b) Classification annotated infrared thermal imaging image

4.2 Dataset preprocessing and configuration file preparation

To prepare for model training, the FLIR Thermal Starter dataset must undergo preprocessing. This involves converting the annotations from JSON format to the YOLO format and organizing the dataset according to the YOLOv5 training file structure. Additionally, the YOLOv5 code library needs to be set up. Within the YOLOv5 directory, the model folder contains configuration files for various model versions: s, m, l, and x. The architecture size increases with the version, resulting in longer training times. For this study, to ensure real-time performance, the version 's' is selected, which corresponds to the *yolov5s.yaml* configuration. The model file is named *model_Yolov5s.yaml*, with modified parameters.

Additionally, the *model_data.yaml* file is prepared, which includes information on the dataset location, the number of categories, and the names of the training and validation sets.

4.3 Parameter setting and model training

The first step involves downloading the pre-trained model corresponding to the YOLOv5 source code from the official website. The second step is to perform model training, with the training parameters specified in Table 2.

Table 2. Training parameter settings

| Parameter | Value | Description |
|--------------|--------------------|---|
| img | 640 | width and height of the input image |
| batch-size | 32 | Batch size |
| epochs | 300 | Training iteration algebra |
| data | model_data.yaml | Files for storing training and testing data |
| cfg | model_yolov5s.yaml | Configuration file for storing model structure |
| cache-images | true | Caching images can accelerate training speed |
| resume | true | Restore the recently saved model and start training |
| nosave | false | Save only the final checkpoint |
| notest | true | Only test the last epoch |
| noautoanchor | false | Adaptive anchoring box |
| multi-scale | true | Input image multi-scale training to prevent model overfitting |
| single-cls | false | The output of the model is a single class training set |

5. EXPERIMENTAL RESULTS AND ANALYSIS

5.1 Evaluating indicator

For classification problems, the performance of the classifier is typically evaluated using the concepts of True Positive (TP), True Negative (TN), False Positive (FP), and False Negative (FN). TP refers to the number of samples that are actually positive and correctly predicted as positive. TN represents the number of samples that are actually negative and correctly predicted as negative. FP refers to the number of samples that are actually negative but incorrectly predicted as positive. FN represents the number of samples that are actually positive but incorrectly predicted as negative.



(1) Accuracy

Accuracy refers to the ratio of the number of correctly classified samples to the total number of samples, calculated as follows using formula (1):

$$Accuracy = \frac{TP + TN}{TP + TN + FP + FN} \quad (1)$$

(2) Precision and recall

Precision (also known as accuracy in this context) refers to the ratio of correctly detected traffic objects (TP) to the total number of detected objects (TP+FP). It shows how accurate the detected traffic objects are. Recall (also known as sensitivity) refers to the ratio of correctly detected traffic objects (TP) to the total number of actual traffic objects (TP+FN). It indicates how many actual traffic targets have been correctly detected. The accuracy and recall rates are given by formulas (2) and (3) below.

$$Precision = \frac{TP}{TP + FP} \quad (2)$$

$$Recall = \frac{TP}{TP + FN} \quad (3)$$

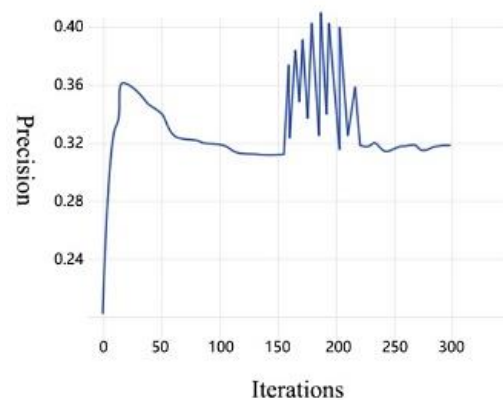
(3) Comprehensive evaluation indicators

The comprehensive evaluation index (F1 score) is the harmonic mean of the accuracy rate and recall rate. The higher the F1 score, the more robust the classification model. As shown in formula (4) below.

$$F1 = 2 \cdot \frac{precision \cdot recall}{precision + recall} \quad (4)$$

5.2 Test result

This study tested 600 infrared thermal images from the FLIR Thermal Starter dataset, which included 2,101 traffic targets such as pedestrians, motor vehicles, and bicycles. After 300 iterations of model training, the detection accuracy reached 90.58%, successfully detecting 1,903 targets. The false detection rate was 5.85%, with 123 false positives, while the missed detection rate was 3.57%, with 75 missed targets. The model achieved a target detection speed of 140 FPS. As shown in Figure 12, accuracy increased with more training iterations, the loss value decreased, and the model began to converge. Both the accuracy and recall rates met the desired requirements.



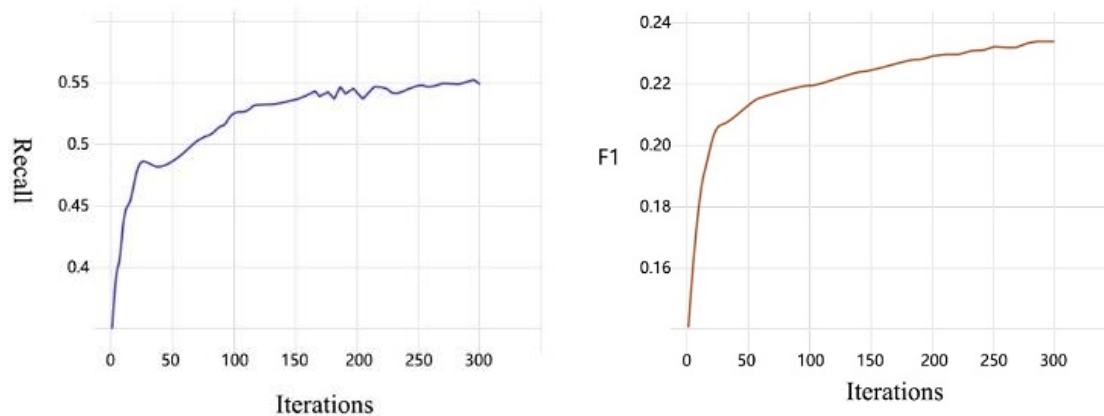


Figure 12. Model training results

Experiments have also demonstrated that the model, after undergoing image preprocessing steps (denoising, enhancement, and ROI extraction), achieves higher classification accuracy and faster detection speed. The comparison of model detection accuracy and speed across different image preprocessing methods is presented in Table 3.

Table 3. Comparison results of different methods

| Algorithm | Image Preprocessing Algorithm | Accuracy | Speed |
|-----------|--|----------|--------|
| YOLO4 | No Image Preprocessing | 0.8032 | 50FPS |
| YOLO4 | Denoising & Enhancement & ROI Extraction | 0.8561 | 65FPS |
| YOLO5 | No Image Preprocessing | 0.8654 | 98FPS |
| YOLO5 | Denoising & Enhancement & ROI Extraction | 0.9058 | 140FPS |

6. SUMMARY

This article highlights the limitations of mainstream automotive sensor technologies in object detection, analyzes the advantages of infrared thermal imaging technology for ADAS system applications, and emphasizes the necessity and technical value of integrating an infrared thermal imager into the sensor suite. The study then combines image preprocessing with the YOLO algorithm to address the challenge of detecting moving objects in complex traffic environments, offering new insights for the practical application of automotive assisted driving systems. Future work will explore the use of color image fusion technology, which combines visible light and infrared thermal images, to enhance traffic detection and target recognition. This approach aims to improve the speed and accuracy of the target detection system while ensuring its adaptability across various scenarios.

ACKNOWLEDGMENT

This work is supported by the the research result of scientific research project of Zhejiang Business College "Research on pedestrian target detection method based on visible light and infrared dual-mode image fusion" in 2023 (Grant No.: SZYZD202304).

REFERENCES

- [1] Gouribhatla, R., Pulugurtha, S.S. (2022). Drivers' behavior when driving vehicles with or without advanced driver assistance systems: A driver simulator-based study. *Transportation Research Interdisciplinary Perspectives*, 13: 100545. <https://doi.org/10.1016/J.TRIP.2022.100545>
- [2] Brijs, T., Mauriello, F., Montella, A., Galante, F., Brijs, K., Ross, V. (2022). Studying the effects of an advanced driver-assistance system to improve safety of cyclists overtaking. *Accident Analysis & Prevention*, 174, 106763. <https://doi.org/10.1016/j.aap.2022.106763>
- [3] Ghahremannezhad, H., Shi, H., Liu, C. (2023). Object detection in traffic videos: A survey. *IEEE Transactions on Intelligent Transportation Systems*, 24(7): 6780-6799. <https://doi.org/10.1109/TITS.2023.3258683>
- [4] Fernandes, A.M., Utkin, A.B., Chaves, P. (2022). Automatic early detection of wildfire smoke with visible light cameras using deep learning and visual explanation. *IEEE Access*, 10: 12814-12828. <https://doi.org/10.1109/ACCESS.2022.3145911>
- [5] Holzhüter, H., Bödewadt, J., Bayesteh, S., Aschinger, A., Blume, H. (2023). Technical concepts of automotive LiDAR sensors: A review. *Optical Engineering*, 62(3): 031213-031213. <https://doi.org/10.1117/1.OE.62.3.031213>
- [6] Yan, X., Yang, Y., Lu, G. (2021). A target detection algorithm based on faster R-CNN. In *Artificial Intelligence for Communications and Networks: Second EAI International Conference, AICON 2020, Virtual Event*, pp. 502-509. https://doi.org/10.1007/978-3-030-69066-3_44
- [7] Ou, J., Wang, J., Xue, J., Wang, J., Zhou, X., She, L., Fan, Y. (2022). Infrared image target detection of substation electrical equipment using an improved faster R-CNN. *IEEE Transactions on Power Delivery*, 38(1): 387-396. <https://doi.org/10.1109/TPWRD.2022.3191694>
- [8] Zhou, X., Jiang, L., Hu, C., Lei, S., Zhang, T., Mou, X. (2022). YOLO-SASE: An improved YOLO algorithm for the small targets detection in complex backgrounds. *Sensors*, 22(12): 4600. <https://doi.org/10.3390/s22124600>
- [9] Nawaz, M., Khalil, M., Shehzad, M.K. (2023). MIYOLO: Modification of Improved YOLO-v3. *IETE Journal of Research*, 69(11): 8036-8044. <https://doi.org/10.1080/03772063.2022.2048709>

- [10] Kang, S.H., Park, J.S. (2023). Aligned matching: Improving small object detection in SSD. *Sensors*, 23(5): 2589. <https://doi.org/10.3390/s23052589>
- [11] Fish, F., Bras, B. (2022). Sustainable design of advanced driver assistance systems based on optimization and empirical studies on full-size light-duty pickup trucks. *Procedia CIRP*, 105: 67-72. <https://doi.org/10.1016/J.PROCIR.2022.02.012>
- [12] James, S.M., James, L. (2023). The impact of 12 h night shifts on nurses' driving safety. *Nursing Reports*, 13(1): 436-444. <https://doi.org/10.3390/nursrep13010040>
- [13] Choi, C.H., Han, J., Cha, J., Choi, H., Shin, J., Kim, T., Oh, H.W. (2024). Contrast enhancement method using region-based dynamic clipping technique for LWIR-based thermal camera of night vision systems. *Sensors*, 24(12): 3829. <https://doi.org/10.3390/S24123829>
- [14] Mirka, B., Stow, D.A., Paulus, G., Loerch, A.C., Coulter, L.L., An, L., Pflüger, L.S. (2022). Evaluation of thermal infrared imaging from uninhabited aerial vehicles for arboreal wildlife surveillance. *Environmental Monitoring and Assessment*, 194(7): 512. <https://doi.org/10.1007/s10661-022-10152-2>
- [15] Jameel, S.K., Majidpour, J. (2022). Generating spectrum images from different types—Visible, Thermal, and Infrared Based on Autoencoder Architecture (GVTI-AE). *International Journal of Image and Graphics*, 22(1): 2250005. <https://doi.org/10.1142/S021946782250005X>
- [16] Pinchon, N., Cassignol, O., Nicolas, A., Bernardin, F., Leduc, P., Tarel, J.P., Brunet, J. (2019). All-weather vision for automotive safety: Which spectral band? In *Advanced Microsystems for Automotive Applications 2018: Smart Systems for Clean, Safe and Shared Road Vehicles 22nd*, pp. 3-15. https://doi.org/10.1007/978-3-319-99762-9_1
- [17] Neumann, T. (2024). Analysis of advanced driver-assistance systems for safe and comfortable driving of motor vehicles. *Sensors*, 24(19): 6223. <https://doi.org/10.3390/S24196223>
- [18] Zeng, X., Xu, J., Gao, X. (2020). A potential method for the nonuniformity correction and noise removal of infrared thermal image. *Acta Physica Polonica, A*, 137(6): 1055-1060. <https://doi.org/10.12693/APhysPolA.137.1055>
- [19] Akula, N.V.A., Sardana, H.K. (2018). Optimized bag of features framework for object recognition in thermal infrared images. *Journal of Electronic Imaging*, 27(6): 063017-063017. <https://doi.org/10.1117/1.JEI.27.6.063017>
- [20] Tan, Y., Qin, J. (2022). An intelligent image denoising method using weighted multi-scale CB morphological filter algorithm. *International Journal of Information Technology and Management*, 21(4): 359-368. <https://doi.org/10.1504/IJITM.2022.10051594>
- [21] Li, Y., Li, Z., Siddique, A., Liu, Y. (2025). Contrast enhancement algorithm for infrared images based on multiscale difference of morphological reconstruction. *Optics & Laser Technology*, 181: 111728. <https://doi.org/10.1016/J.OPTLASTEC.2024.111728>
- [22] Im Choi, J., Tian, Q. (2025). Saliency and location aware pruning of deep visual detectors for autonomous driving. *Neurocomputing*, 611: 128656. <https://doi.org/10.1016/j.neucom.2024.128656>